To be published in Optics Express:

Title:	Controllable duration and repetition-rate picosecond pulses from a record-average-power OP-GaAs OPO
Authors:	Qiang Fu,Yudi Wu,Sijing Liang,Peter Shardlow,David Shepherd,Shaif-Ul Alam,Lin Xu,David Richardson
Accepted:	22 September 20
Posted	22 September 20
DOI:	https://doi.org/10.1364/OE.402360

Controllable duration and repetition-rate picosecond pulses from a high-average-power OP-GaAs OPO

QIANG. FU, YUDI. WU, SIJING. LIANG, PETER. C. SHARDLOW, DAVID. P. SHEPHERD, SHAIF-UL. ALAM, LIN. XU*, AND DAVID. J. RICHARDSON

Optoelectronics Research Centre, University of Southampton, SO17 1BJ, UK
* l.xu@soton.ac.uk

Abstract: We report an orientation-patterned gallium arsenide (OP-GaAs) optical parametric oscillator (OPO) offering a high degree of temporal flexibility with controllable pulse repetition rates from 100 MHz to 1 GHz and pulse durations from ~95 ps to ~1.1 ns. The maximum average power of 9.2-W signal (3.3 μm) and 4.5-W idler (4.9 μm) was obtained at a repetition rate of 100 MHz and a pulse duration of ~95 ps, with a pump power of 34.3 W and at a slope efficiency of 45.4%. The corresponding total average output power of 13.7 W is the highest power achieved to date from an OP-GaAs OPO, to the best of our knowledge.

1. Introduction

Pulsed mid-IR lasers are of great interest for spectroscopy, chemical sensing and biomedicine [1, 2], and output power, pulse repetition rate and pulse duration are key parameters for many applications. For example, in mid-IR chemical sensing, high output power improves the signal-to-noise ratio associated with long-range measurement and a high pulse repetition rate reduces the signal processing time for high-speed chemical detection [3]. For biological applications, controllable mid-IR pulse durations allow the investigation of pulse-duration-dependent laser ablation [4]. In addition, flexible temporal properties could be useful for dynamic studies [5] and performance optimization of material processing [6, 7] and microscopy [8]. Therefore, pulsed mid-IR lasers with high powers and high degrees of temporal flexibility are widely desirable.

Mid-IR OPOs are a promising solution, offering high powers and wide wavelength tunability, with temporal properties that are substantially determined by their pump sources. High-repetition-rate OPOs can be achieved by harmonic pumping, as has been previously reported in [9-12], but these demonstrations were only for fixed pulse durations. In order to achieve flexible repetition rate and pulse duration simultaneously, amplified gain-switched laser diodes (GSLDs) can be considered as ideal pump sources, and they have previously been used to pump a variable repetition rate (115 – 918 MHz) periodically-poled-lithium-niobate (PPLN) -based picosecond OPO by allowing one or more pulses to circulate within the OPO cavity while still achieving synchronous pumping [13]. However, this demonstration was still operated at a fixed pump pulse duration (~17 ps) and at relatively short wavelengths (no longer than 4.4 μm) due to the short transmission range of the PPLN. OP-GaAs, as a non-oxide crystal, is better suited for longer-wavelength mid-IR OPOs due to its broad transparency (0.9 μm – 17 μm) and it also has a larger nonlinear coefficient (94 pm/V) [14] in comparison to PPLN. We previously reported a high-peak-power OP-GaAs optical parametric generator and amplifier (OPG/A) pumped by an amplified GSLD [15]. However, the average output powers were relatively low (maximum 1.33 W) due to the low repetition rate (1 MHz). We then demonstrated a high-average-power OP-GaAs OPO operating at a higher repetition rate (100 MHz) [16], but observed that a thermally induced power roll-off limited the maximum output power to 9.7 W.

Here we report a maximum 13.7-W mid-IR OP-GaAs OPO, without any power roll-off meaning that the output power is only limited by the available pump power, and with flexible repetition rates and controllable pulse durations benefiting from the flexible temporal properties of the amplified GSLD pump. The OPO was first investigated at a fundamental repetition rate of 100 MHz, corresponding to one pulse circulating within the cavity, and a 95-ps pump pulse. Operating at the fundamental frequency of the cavity, the OPO delivered the maximum output power, consisting of 9.2 W signal and 4.5 W idler at wavelengths of 3.3 μm and 4.9 μm, respectively. The corresponding maximum peak powers for signal and idler were estimated to be 968 W and 473 W, respectively. Thermal management, here by water cooling, was found to be essential as crystal damage was observed at a pump power of ~32 W (~1.3 mJ/cm^2) without this. By controlling the electrical drive signal to the GSLD, and without the need to alter the following fiber amplifier chain, a variable pulse repetition-rate and duration OPO was realized with repetition rates from 100 MHz to 1 GHz, by increasing the number of circulating pulses within the cavity from 1 to 10, and with pulse durations from ~95 ps – ~1.1 ns. The OPO offered >3 W total average output power for all the demonstrated repetition rates and pulse durations. To the best of our knowledge, this is the first demonstration of high-power, controllable duration and repetition-rate, ultrashort pulses from an OPO.

2. Experimental setup

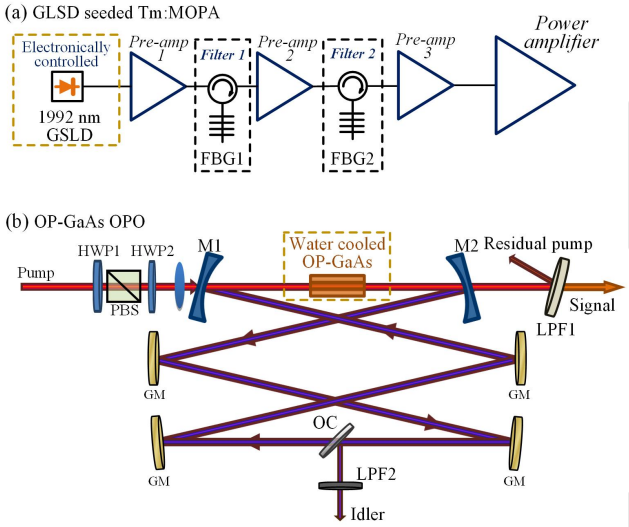

Fig. 1. (a) Schematic of the setup of the OPO pump – a GSLD-seeded Tm:MOPA system, GSLD: gain-switched laser diode; pre-amp: pre-amplifier; FBG: fiber Bragg grating. (b) Setup of OP-GaAs OPO, HWP: half-wave plate, PBS: polarization beam splitter; M1,2: dielectric-coated mirror 1,2; GM: gold mirror; LPF: long-pass filter; OC: output coupler.

Fig. 1 (a) shows the experimental setup of the pump system for the OP-GaAs OPO, which was a thulium-doped fiber master oscillator power amplifier (Tm:MOPA) system seeded by a 1992-nm GSLD (Eblana Photonics), similar to that reported in [16]. The temporal properties of the Tm:MOPA system were controlled by the electronically-driven GSLD whereas its spectral bandwidth was constrained by two FBG-based spectral filters with a bandwidth of 0.2 nm and 0.5 nm for Filter 1 and 2 respectively. The pumping system was operated in three different regimes – fundamental operation regime, controllable repetition rate regime, and controllable pulse duration regime. A repetition rate of 100 MHz and a final output pulse duration of 95 ps was considered as the fundamental operation regime. By manipulating the

electrical pulses imposed on the GSLD, the repetition rate of the pump system can be varied from 100 MHz to 1 GHz for a fixed pulse duration of 95 ps, and its pulse duration can be changed from 95 ps to 1.1 ns for a fixed repetition rate of 100 MHz, whilst maintaining the same average output power. It should be noted that the pump spectral bandwidths for the three operation regimes were different (maximum 0.4 nm for fundamental operation regime), but were all well within the acceptance bandwidth for the OP-GaAs crystal (~1.6 nm, calculation based on the assumption of a monochromatic idler wave). All other output characteristics, such as beam quality (M^2=1.2), and polarization extinction ratio (14 dB) remained the same in the different operation regimes.

Fig. 1 (b) shows a schematic of the synchronously pumped OP-GaAs OPO. A half-wave plate (HWP1) and a polarization beam splitter (PBS) were used to control the pump power, whilst the other half-wave plate (HWP2) was employed to rotate the pump polarization. The pump beam was focused by an anti-reflection (AR) coated calcium fluoride lens (f=200 mm) into the OP-GaAs crystal (BAE Systems) with a beam waist of ~93 μm ($1/e^2$ radius of intensity). The OP-GaAs had a period of 57 μm and was 20-mm long, 5-mm wide, and 1-mm thick. It was anti-reflection (AR) coated at pump, signal and idler wavelengths (AR>99%). In order to mitigate thermal effects, it was mounted on a water-cooled plate with a cooling temperature of 17.5°C. The OPO cavity was an idler-resonant ring cavity designed to generate high-beam-quality idler output, such that it would be compatible with mid-IR fiber-based power delivery [17]. The cavity had two plane-concave dielectric-coated mirrors (M1, M2, high-reflectivity >99.5% at idler, AR>98% at pump, and ~18% reflectivity at signal) and four plane-plane gold-coated mirrors. M1 and M2 both had a radius of curvature of 250 mm and were separated by 270 mm, leading to a calculated idler beam waist of 92 μm in the centrally located crystal. The total optical cavity length of 3 m was set to match the repetition rate of the fundamental operation regime (100 MHz). Note that no active stabilization of the OPO cavity was required due to the relatively long pump pulses (at least 95 ps) used in this work. Two different output couplers, a coated calcium fluoride plate (OC1, Thorlabs, BSW511R, reflectivity ~31% at idler) and a pellicle beam splitter (OC2, Thorlabs, BP108, reflectivity ~3% at idler), were investigated for extraction of the idler from the cavity. Two long pass filters were used to pass the generated signal (LPF1, transmission 91%±1%) and idler (LPF2, transmission 80%±1%), respectively, and to reflect unwanted residual pump (reflection >99%). The quoted output powers of the signal and idler in the following section were calculated from the direct measurements and by considering the corresponding LPF loss.

3. Results and discussions

3.1 Fundamental operation regime of the high-average-power OPO

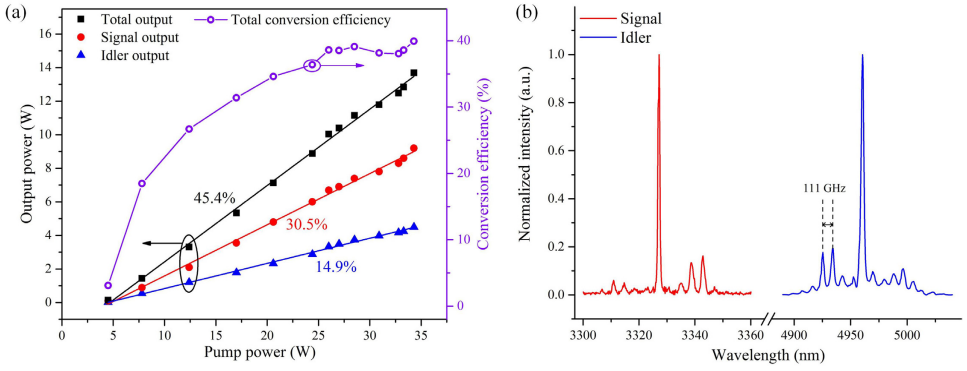

Fig. 2. (a) Output powers and total conversion efficiencies for the fundamental operation. (b) Signal and idler spectra at the maximum output power for the fundamental operation.

The OPO was operated at a repetition rate of 100 MHz and a pump pulse duration of 95 ps in the fundamental operation regime. To maximize the output power, the polarization of the pump beam was set along the [111] crystallographic axis of the OP-GaAs [18]. Fig. 2 (a) shows the output powers and conversion efficiencies for the OPO fundamental operation regime with OC1 in the cavity. An OPO oscillation threshold of 4.5 W was observed at signal and idler wavelengths of ~3.3 μm and ~4.9 μm, respectively. A slope efficiency of 45.4% and a maximum total OPO average power of 13.7 W were achieved at a maximum pump power of 34.3 W. The corresponding signal and idler maximum output powers were 9.2 W and 4.5 W from the OPO, respectively, with extracted powers of 8.4 W (signal) and 3.6 W (idler) after the LPFs. Assuming the pulse durations of the signal and idler pulses were similar to those of pump pulses (95 ps), the peak powers of the generated signal and idler pulses were 968 W and 473 W, respectively. A total maximum optical-to-optical OPO conversion efficiency of ~40% was obtained without any obvious roll-off, which indicates that the OPO output power was only limited by the currently available pump power. This should be compared to our previous report at the same pump power level but implemented without water cooling, where a thermally induced roll-off was observed [16]. Fig. 2 (b) plots the signal and idler spectra at the maximum output power for the fundamental operation regime of the OPO with OC1 in the cavity (their corresponding pump spectra is shown in Fig. 4 (black line)). The spectra were measured by an optical spectrum analyzer (Bristol Instruments 771 series, 0.15 nm resolution) and a monochromator (Bentham TMc300, 1 nm resolution) combined with an InSb detector (Elector-Optical Systems IS030-LN4) for signal and idler, respectively. A peak wavelength of 3327 nm and 4960 nm was obtained for signal and idler with a corresponding 3-dB bandwidth of 0.8 nm (0.7 cm^{-1}) and 3 nm (1.2 cm^{-1}), respectively. Such bandwidths and observed spectral side bands originated from the etalon effects of OC1, and the measured spacing of the idler spectral peaks of 111 GHz (Fig. 2 (b)) corresponded to a similar calculated free spectral range of 107 GHz for OC1. The small discrepancy probably originated from inaccuracy in the thickness of OC1 and the beam incident angle. By using a pyroelectric scanning-slit beam profiler (Ophir, NanoScan), the beam qualities for the generated outputs were measured with M^2 values for signal and idler of 1.2 and 1.1, respectively, at a pump power of 15 W; and 1.5 and 1.1, respectively, at the maximum pump power of 34.3 W.

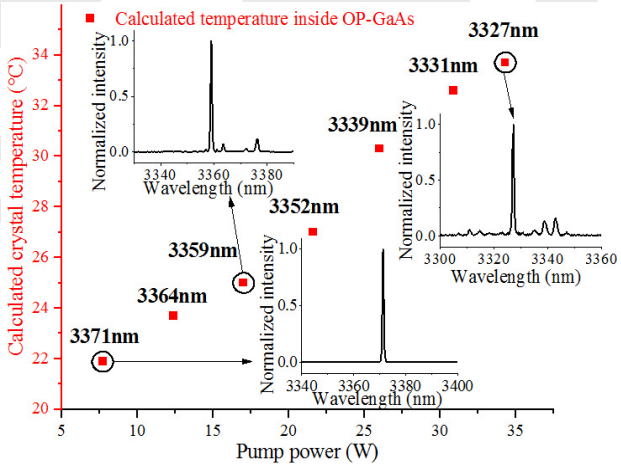

Fig. 3. Measured signal central wavelength shift at different pump powers and their corresponding calculated temperatures inside the OP-GaAs sample. Insets: example spectra at signal peak wavelengths of 3371, 3359, and 3327 nm.

Although the water-cooling temperature was fixed, we observed that the OPO signal wavelength shifted with average power, which indicated a temperature change inside the

crystal, as shown in Fig. 3. The temperatures for the different signal peak wavelengths were then calculated based on the Sellmeier equations for the OP-GaAs crystal [19]. A theoretical temperature of 33.7°C was estimated at the maximum output power. The tuning ability of the OPO was currently limited by the fixed water-cooling temperature and the OP-GaAs period, however, it could be extended by, for example, choosing an OP-GaAs crystal with fan-out designed periods. Note that in an experiment without using the water cooling, thermally induced OP-GaAs crystal damage was observed at a pump power of ~32 W (~1.3 mJ/cm^2) under long-term operation. We note that this was a single observation and no systematic investigation of damage threshold has been performed to date. We believe high-average-power-induced thermal effects were responsible for this crystal damage rather than the fluence, as no damage was seen at a much higher fluence of 18 mJ/cm^2 but at a much lower average power, and at a similar pulse duration of ~80 ps, in our previously reported OP-GaAs OPG/A experiments [15]. Further studies of OP-GaAs crystal damage mechanisms are now underway.

3.2 Controllable repetition-rate OPO – 100 MHz to 1 GHz

By changing the repetition rate of the pump (in harmonics of the fundamental operation), a controllable repetition-rate OPO can be achieved with a corresponding change in the number of pulses circulating within the (unchanged) cavity. Here, an idler-resonant OP-GaAs OPO operating at ten different repetition rates, stepping from 100 MHz to 1 GHz (1 to 10 idler pulses in the cavity, respectively) was experimentally achieved.

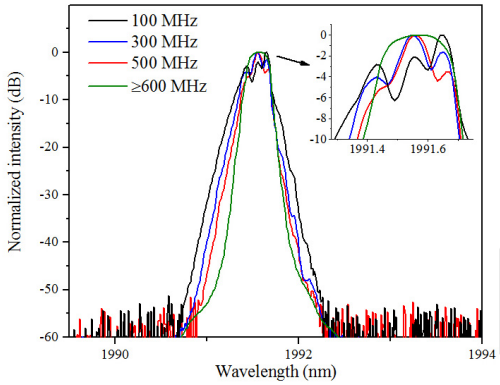

Fig. 4. Spectra of the GSLD-seeded Tm:MOPA at maximum output power but different repetition rates (0.05 nm resolution). Inset shows the enlarged details of the spectra at the peak.

Benefiting from GSLD seeding, the repetition rate of the pump system can easily be changed by modifying the repetition rate of its electrical drive pulses from 100 MHz to 1 GHz. Regardless of the variations of the pulse repetition rate, the final average output power from the following Tm:MOPA system remained constant. Consequently, different peak powers at different repetition rates, caused different degrees of spectral broadening in the power amplifier (Fig. 1 (a)). Fig. 4 shows the spectra of the Tm:MOPA system at the same output power (39 W) and pulse duration (95 ps), but at different repetition rates. Self-phase-modulation-induced spectral features were seen for repetition rates below 600 MHz but were not observable for repetition rates above 600 MHz, however, the spectral bandwidths at all repetition rates were all within the OPO pump acceptance requirement.

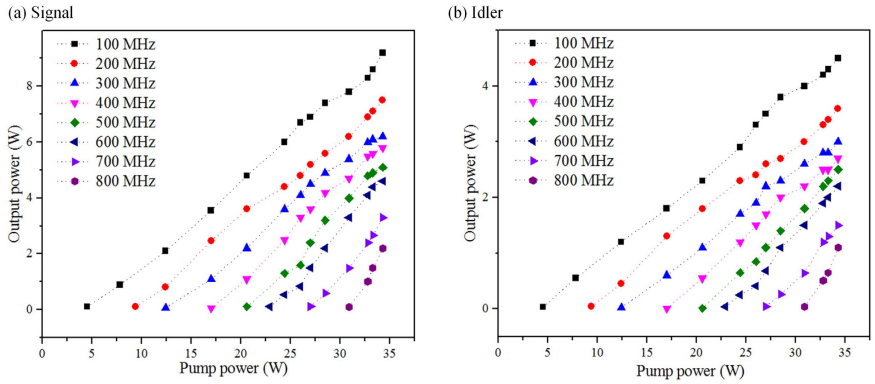

Fig. 5. Signal (a) and idler (b) output powers at 100 – 800 MHz repetition rates.

With OC1 employed for the OPO, a controllable repetition-rate from 100 to 800 MHz was realized, and the signal and idler powers are presented in Fig. 5. The average-power pump thresholds increased at higher repetition rates due to the lower peak powers. At 800-MHz repetition rate, 2.2 W and 1.1 W of signal and idler output power were obtained at a maximum pump power of 34.3 W, respectively. Repetition rates higher than 800 MHz OPO were difficult to achieve when using OC1. To reduce the pump threshold for such high repetition rates, OC2 was chosen to give a lower intra-cavity loss and to extract ~3% of idler power out of the cavity. At an oscillation threshold of 27 W, a 1-GHz OP-GaAs OPO was successfully realized. Although only 27 mW of idler was extracted from the cavity, 3.5 W of signal output power was obtained at the maximum pump power. Spectra of the signal and idler at maximum output power at 1 GHz were characterized, as presented in Fig. 6 (a). The central signal and idler wavelengths of 3356 nm and 4897 nm were measured with a 3-dB bandwidth of 1.3 nm (1.1 cm^{-1}), and 4 nm (1.7 cm^{-1}), respectively. Due to the thin-film nature of OC2, no etalon effect and no associated side peak spectra were observed. The total output powers (signal + idler) for the variable repetition rate OPO are summarized in Fig. 6 (b) with more than 3 W achieved at all repetition rates (100 MHz – 1 GHz).

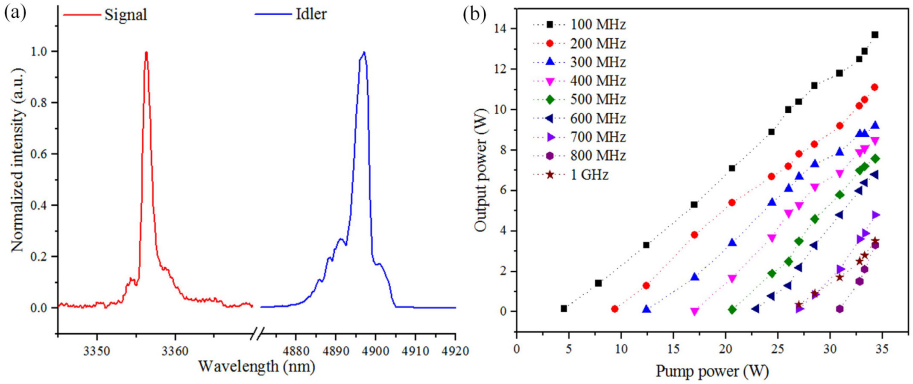

Fig. 6. (a) Signal and idler spectra at a repetition rate of 1 GHz. (b) Total output powers for the variable repetition-rate OPO.

3.3 Controllable pulse-duration OPO – 95 ps to 1.1 ns

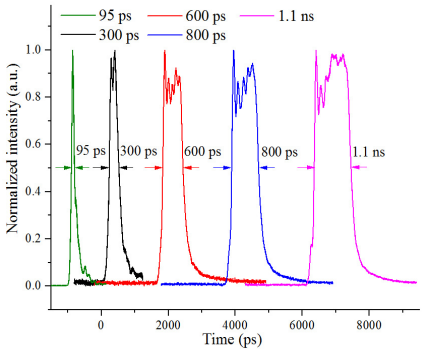

Fig. 7. Example pulses from the Tm:MOPA with a pulse duration of 95, 300, 600, 800 ps and 1.1. ns.

At a fixed repetition rate of 100 MHz, a controllable pulse-duration OPO was realized with pump pulse durations ranging from 95 ps to 1.1 ns, profiting again from the ease of tailoring the temporal properties of the GSLD-seeded Tm:MOPA pump system. By adjusting the electrically driven pulse durations, as well as controlling the spectral filters (FBG1 and FBG2 in Fig. 1), at a constant output power (39 W), continuously duration-tunable pulses from the Tm:MOPA were achieved (95 ps to 1.1 ns). For the controllable pulse-duration OPO, the two FBG-based filters not only narrowed the spectral bandwidth, but also have the effect of removing the leading spike of the gain-switched pulse in the temporal domain. Example pulse profiles, 95, 300, 600, 800 ps, and 1.1 ns, are presented in Fig. 7 with the seed diode driven by 430, 680, 990 ps, 1.2 ns and 1.5 ns electronic pulses, respectively. The pump pulses were characterized by a >12.5-GHz-bandwidth photodetector (EOT 5000F) together with a communication signal analyzer (50-GHz bandwidth, Tektronix CSA 803).

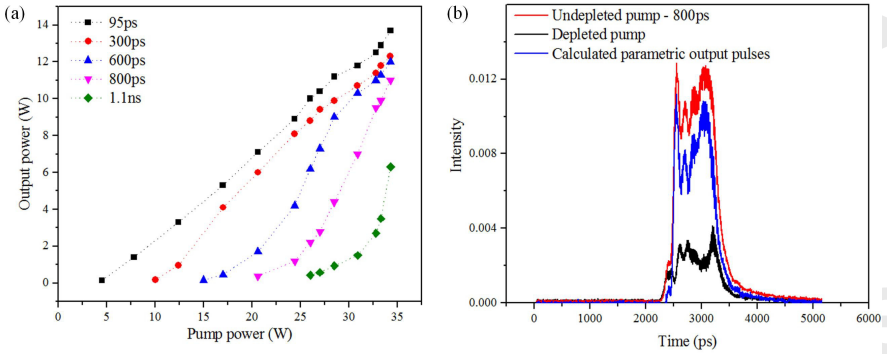

Fig. 8. (a) Total output powers from the variable pulse-duration OPO. (b) An example depleted pump shape compared with its original shape at a pulse duration 800 ps. Blue line shows the calculated parametric output pulses.

Fig. 8 (a) plots the generated total output powers (signal + idler) of the controllable pulse-duration OPO at a repetition rate of 100 MHz with OC1 in the cavity. At example pump pulse durations of 300, 600, 800 ps and 1.1 ns, the output powers for the signal were 8.4, 8.2, 7.6, and 4.4 W respectively, while for the idler these were 3.9, 3.8, 3.4 and 1.9 W respectively. At the longest pump pulse duration of 1.1 ns, a total OPO output power of 6.3 W was obtained, and the OPO did not oscillate for pulses longer than 1.1 ns due to the increased threshold power requirement. Due to the fact that the pump pulse shapes were not purely rectangular for different pulse durations (Fig. 7), we would expect that the oscillation threshold and output characteristics would be slightly affected by the small change in pulse shape. The pulse shapes of the generated signal and idler were not characterized due to the lack of suitable,

commercially available, high-speed, mid-IR photodetectors and the lack of long-scan-range mid-IR autocorrelators in our labs. Therefore, they were assumed to have similar durations to their corresponding pumps as a consequence of the nonlinear parametric process [20-22]. Fig. 8 (b) depicts pulse profiles of the depleted pump pulse compared with the undepleted pump pulse at a duration of 800 ps, which shows relatively constant depletion across the pump pulse. The blue line is an approximation for the temporal shape of the generated parametric pulses and obtained by calculating the difference between the depleted and undepleted pump pulse.

4. Conclusion

In conclusion, a high-average-power controllable pulse repetition-rate and duration OPO has been demonstrated based on OP-GaAs. With a fundamental pump pulse repetition rate of 100 MHz and pulse duration of 95 ps, a maximum total average power of 13.7 W, including 9.2 W signal (3.3 μm) and 4.5 W idler (4.9 μm), was obtained. Thermal management was essential for such average power operation of OP-GaAs as crystal damage was observed at a pump power of ~32 W (~1.3 mJ/cm^2) without water cooling. By manipulating the temporal properties of the pump pulses, the OP-GaAs OPO can offer variable repetition rates from 100 MHz to 1 GHz and controllable pulse durations from ~95 ps to ~1.1 ns. At least 3-W total output power was achieved for all demonstrated repetition rates and pulse durations. To the best of our knowledge, this is the first demonstration of a mid-IR OPO offering high powers and a high degree of simultaneous flexibility on repetition rate and pulse duration.

Funding

EPSRC AirGuide Photonics Programme Grant (Grant EP/P030181/1)

Acknowledgements

The authors thank Dr. Peter G. Schunemann from BAE Systems for growing the OP-GaAs crystals and Prof. W.A. Clarkson from the ORC for providing the large-mode-area thulium doped fibers. Qiang Fu thanks the China Scholarship Council for financial support of his PhD. The data from the figures can be found in https://doi.org/10.5258/SOTON/D1504.

Disclosures

The authors declare no conflicts of interests.

References

1. I. T. Sorokina, and K. L. Vodopyanov, *Solid-State Mid-Infrared Laser Sources*, Springer Science & Business Media (2003).
2. V. A. Serebryakov, É. V. Boĭko, N. N. Petrishchev, and A. V. Yan, "Medical applications of mid-IR lasers. Problems and prospects," J. Opt. Technol. **77**(1), 6-17 (2010).
3. C. Gu, Z. Zuo, D. Luo, D. Peng, Y. Di, X. Zou, L. Yang, and W. Li, "High-repetition-rate femtosecond mid-infrared pulses generated by nonlinear optical modulation of continuous-wave QCLs and ICLs," Opt. Lett. **44**(23), 5848-5851 (2019).
4. M. A. Mackanos, D. M. Simanovskii, K. E. Schriver, M. S. Hutson, C. H. Contag, J. A. Kozub, and E. D. Jansen, "Pulse-duration-dependent mid-infrared laser ablation for biological applications," IEEE J. Sel. Top. Quant. **18**(4), 1514-1522 (2012).
5. C. B. Schaffer, N. Nishimura, E. N. Glezer, A. M.-T. Kim, and E. Mazur, "Dynamics of femtosecond laser-induced breakdown in water from femtoseconds to microseconds," Opt. Express **10**(3), 196-203 (2002).
6. P. E. Schrader, R. L. Farrow, D. A. Kliner, J.-P. Fève, and N. Landru, "High-power fiber amplifier with widely tunable repetition rate, fixed pulse duration, and multiple output wavelengths," Opt. Express **14**(24), 11528-11538 (2006).

7. J. Cheng, C.-s. Liu, S. Shang, D. Liu, W. Perrie, G. Dearden, and K. Watkins, "A review of ultrafast laser materials micromachining," Optics & Laser Technology **46**(88-102 (2013).
8. K. Charan, B. Li, M. Wang, C. P. Lin, and C. Xu, "Fiber-based tunable repetition rate source for deep tissue two-photon fluorescence microscopy," Biomedical optics express **9**(5), 2304-2311 (2018).
9. D. T. Reid, C. McGowan, W. Sleat, M. Ebrahimzadeh, and W. Sibbett, "Compact, efficient 344-MHz repetition-rate femtosecond optical parametric oscillator," Opt. Lett. **22**(8), 525-527 (1997).
10. B. Ruffing, A. Nebel, and R. Wallenstein, "All-solid-state cw mode-locked picosecond KTiOAsO4 (KTA) optical parametric oscillator," Appl. Phys. B **67**(5), 537-544 (1998).
11. J. Jiang, and T. Hasama, "Harmonic repetition-rate femtosecond optical parametric oscillator," Appl. Phys. B **74**(4), 313-317 (2002).
12. A. Esteban-Martin, O. Kokabee, K. Moutzouris, and M. Ebrahim-Zadeh, "High-harmonic-repetition-rate, 1 GHz femtosecond optical parametric oscillator pumped by a 76 MHz Ti:sapphire laser," Opt. Lett. **34**(4), 428-430 (2009).
13. F. Kienle, K. K. Chen, S.-u. Alam, C. B. E. Gawith, J. I. Mackenzie, D. C. Hanna, D. J. Richardson, and D. P. Shepherd, "High-power, variable repetition rate, picosecond optical parametric oscillator pumped by an amplified gain-switched diode," Opt. Express **18**(8), 7602-7610 (2010).
14. P. G. Schunemann, "New nonlinear optical crystals for the mid-infrared," in OSA Technical Digest (online), *Advanced Solid State Lasers Conference (ASSL)* AM2A.2 (2015).
15. L. Xu, Q. Fu, S. Liang, D. P. Shepherd, D. J. Richardson, and S. U. Alam, "Thulium-fiber-laser-pumped, high-peak-power, picosecond, mid-infrared orientation-patterned GaAs optical parametric generator and amplifier," Opt. Lett. **42**(19), 4036-4039 (2017).
16. Q. Fu, L. Xu, S. Liang, P. C. Shardlow, D. P. Shepherd, S.-u. Alam, and D. J. Richardson, "High-average-power picosecond mid-infrared OP-GaAs OPO," Opt. Express **28**(4), 5741-5748 (2020).
17. A. Ventura, J. G. Hayashi, J. Cimek, G. Jasion, P. Janicek, F. B. Slimen, N. White, Q. Fu, L. Xu, H. Sakr, N. V. Wheeler, D. J. Richardson, and F. Poletti, "Extruded tellurite antiresonant hollow core fiber for Mid-IR operation," Opt. Express **28**(11), 16542 (2020).
18. K. L. Vodopyanov, O. Levi, P. S. Kuo, T. J. Pinguet, J. S. Harris, M. M. Fejer, B. Gerard, L. Becouarn, and E. Lallier, "Optical parametric oscillation in quasi-phase-matched GaAs," Opt. Lett. **29**(16), 1912-1914 (2004).
19. T. Skauli, P. S. Kuo, K. L. Vodopyanov, T. J. Pinguet, O. Levi, L. A. Eyres, J. S. Harris, M. M. Fejer, B. Gerard, L. Becouarn, and E. Lallier, "Improved dispersion relations for GaAs and applications to nonlinear optics," Journal of Applied Physics **94**(10), 6447-6455 (2003).
20. O. Kokabee, A. Esteban-Martin, and M. Ebrahim-Zadeh, "Efficient, high-power, ytterbium-fiber-laser-pumped picosecond optical parametric oscillator," Opt. Lett. **35**(19), 3210-3212 (2010).
21. L. Xu, H.-Y. Chan, S.-u. Alam, D. J. Richardson, and D. P. Shepherd, "High-energy, near- and mid-IR picosecond pulses generated by a fiber-MOPA-pumped optical parametric generator and amplifier," Opt. Express **23**(10), 12613-12618 (2015).
22. G. Marchev, P. Dallocchio, F. Pirzio, A. Agnesi, G. Reali, V. Petrov, A. Tyazhev, V. Pasiskevicius, N. Thilmann, and F. Laurell, "Sub-nanosecond, 1–10 kHz, low-threshold, non-critical OPOs based on periodically poled KTP crystal pumped at 1,064 nm," Appl. Phys. B **109**(2), 211-214 (2012).